and thickness of the potential barrier. Wilson, Sutin, and Beattie[15-24] have commented on the influence of steric effects for solution-state species. In the case of FeP, for example, steric bulk at the aziridine donor may lengthen the shorter low-spin Fe–N(aziridine) bond but have no effect on the already longer high-spin Fe–N(aziridine) distance. Until very recently, it was just this steric hindrance associated with the aziridine donor that we held as the cause of the relatively fast spin-state interconversion rate observed for FeP. However, single-crystal X-ray structural results obtained for the 3-ethoxy-substituted form of FeP, specifically the benzene solvate $[Fe(3\text{-}OEt\text{-}SalAPA)_2]ClO_4 \cdot C_6H_6$, have shown[52] that this is *not* the explanation. The 300 K X-ray structure and preliminary 128 K X-ray structure of this complex show that there is an appreciable change in the Fe–N(aziridine) bond distance.

In summary, at this time there does *not* seem to be any obvious *intrinsic* factor that leads FeP and the three Maeda[37-39] N_4O_2 ferric spin-crossover complexes to interconvert in the solid state between low-spin and high-spin states faster than the ^{57}Fe Mössbauer time scale, compared to the slow interconversion of other N_4O_2 ferric complexes. It would be interesting to know whether these same N_4O_2 ferric complexes flip spin relatively rapidly in solution as they do in the solid state. In the next two papers in this series we will examine whether there are any effects of *inter*molecular interactions in the solid state upon the rate of spin interconversion.

Acknowledgment. We are grateful for support from NIH Grant HL13652. Partial funding for the Mössbauer equipment came from NSF Grant CHE-78-20727, combined with equal funding from our chemistry department and the Research Board of the University of Illinois. We thank Mark Timken for running EPR spectra of $[Fe(bzpa)_2]PF_6$. Lastly, we are indebted to Prof. C. A. Root of Bucknell University for his guidance in the development of the original synthetic method 1.

Registry No. FeE, 92220-29-6; CoE, 92220-31-0; FeP, 79151-63-6; APA, 1072-65-7; $[Co(SalAEA)_2]Cl$, 92220-32-1; $Fe(ClO_4)_2$, 13933-23-8; ferrous chloride, 7758-94-3; salicylaldehyde, 90-02-8.

Supplementary Material Available: Figure of Mössbauer spectra and listings of microanalytical data (Table I), interplanar spacings (Table II), magnetic susceptibility data (Tables III–VII), Mössbauer parameters (Tables VIII and XI), and EPR parameters (Table XII) (17 pages). Ordering information is given on any current masthead page.

Contribution from the School of Chemical Sciences, University of Illinois, Urbana, Illinois 61801

Dynamics of Spin-State Interconversion and Cooperativity for Ferric Spin-Crossover Complexes in the Solid State. 2. Perturbations of the Fast Spin-Flipping N_4O_2 Complex $[Fe(SalAPA)_2]ClO_4$

WAYNE D. FEDERER[1] and DAVID N. HENDRICKSON*

Received January 13, 1984

The complex $[Fe(SalAPA)_2]ClO_4$ is a ferric spin-crossover complex that flips spin faster than the ^{57}Fe Mössbauer time scale. The effects on the dynamics of spin-state interconversion of various perturbations of this complex are investigated. Solvation to give $[Fe(SalAPA)_2]ClO_4 \cdot CH_2Cl_2$ dramatically affects the temperature at which there are equal amounts of high- and low-spin complexes, shifting this temperature from 295 K for the unsolvated complex to 152 K for the CH_2Cl_2 adduct. The CH_2Cl_2 adduct is still flipping spin faster than the ^{57}Fe Mössbauer time scale at all temperatures; however, the line widths of the two components of the one doublet at each temperature are considerably broader than the corresponding features observed for the unsolvated complex. Grinding $[Fe(SalAPA)_2]ClO_4$ with a mortar and pestle changes the Mössbauer spectra for this complex such that across a broad temperature range (~100–230 K) there are two quadrupole-split doublets present. For one hand-ground sample, the introduction of an external 30-kG field at 5 K in the Mössbauer experiment shows that the "new" doublet is associated with "residual" high-spin ferric complexes. Grinding causes broadening of the low-spin EPR resonances at all temperatures, from which it is inferred that the residual high-spin complexes are located within the same crystallites as the complexes participating in the dynamic spin-state interconversion.

Introduction

In the preceding paper microcrystalline samples of the spin-crossover complex $[Fe(SalAPA)_2]ClO_4$, where SalAPA is the monoanionic Schiff base derived from salicylaldehyde and *N*-(3-aminopropyl)aziridine, were prepared by two different methods and were found to give appreciably different variable-temperature Mössbauer spectra. In the case of one preparative method a microcrystalline sample of $[Fe(SalAPA)_2]ClO_4$ (hereafter called FeP) is obtained directly from the reaction medium. The Mössbauer spectra for this material can be fit reasonably well to one quadrupole-split doublet at all temperatures. It is necessary to recrystallize from a dichloromethane/cyclohexane solution to obtain a microcrystalline sample from the second preparative method. There are clearly two resolved quadrupole-split doublets in each of the Mössbauer spectra at temperatures below ~233 K for this second type of microcrystalline $[Fe(SalAPA)_2]ClO_4$. This is true in spite of the fact that both samples have nearly identical analytical, infrared, and X-ray powder diffraction data. Apparently, in the first case, the FeP complexes are interconverting between low-spin and high-spin states appreciably faster than can be detected by the Mössbauer technique ($k > \sim 10^7\ s^{-1}$) and a *single* population-weighted doublet is seen. It was further suggested in the preceding paper that the microcrystals obtained from the recrystallization method are less crystalline than the microcrystals obtained from the other preparative method. The additional quadrupole doublet could then arise either from FeP complexes in the solid that are persisting in the high-spin state or from FeP complexes that are interconverting somwhat slower than the rapidly interconverting complexes. The increased concentration of defect structure (i.e., dislocations, fissures, cracks on the crystal surfaces, etc.) in the less crystalline FeP sample could be responsible for the presence of the second, "slow" FeP complex.

In this paper an effort has been made to get additional insight into the factors leading to the differences in the Mössbauer characteristics of microcrystalline FeP prepared by the two different methods. More direct evidence was also

(1) 3M Fellowship, 1979–1980. Owens-Corning Fellowship, 1980–1981. Present address: Magnetic Audio/Video Products Division, 3M, St. Paul, MN 55144.

0020-1669/84/1323-3870$01.50/0

sought on the nature of the FeP complexes giving rise to the second quadrupole doublet. Portions of one ^{57}Fe-enriched sample of FeP have been subjected to various "perturbations". These perturbations included preparing an FeP sample solvated with 1 equiv of CH_2Cl_2. This solvated sample was then subjected to the desolvation approach employed in one preparative method. In addition, a portion of the original ^{57}Fe-enriched sample was ground in a mortar and pestle. Mössbauer, EPR, magnetic susceptibility, infrared, and X-ray powder diffraction data have been collected for these various forms of "perturbed" FeP.

Experimental Section

The preceding paper is to be consulted for a description of the physical measurements employed and for general comments about materials. The nature and sensitivity of spin-crossover complexes require that details are given for the specific samples that were studied. Portions of the ^{57}Fe-enriched sample of FeP identified as **U1** were used to prepare many of the compounds described in this paper. The following sample code is used: **G** indicates a mortar and pestle ground sample; **D** indicates a sample that has undergone the CH_2Cl_2/cyclohexane recrystallization followed by desolvation under vacuum. Analytical data are given in Table I.[2]

Compound Preparation. Hand-Ground Samples of FeP. *Caution! FeP is a mildly shock-sensitive perchlorate salt and grinding is a dangerous procedure that is not recommended!*

G1. An electrostatic red-purple powder was obtained after grinding 20 mg of **U1** for ~45 min in a 25-mm diameter mortar.

G2. A product of similar appearance to **G1** resulted from hand grinding of 72 mg of **U2** for ~25 min in a 35-mm mortar.

G3. **G3** was obtained by pulverization of 140 mg of **U3** for ~30 min in an 80-mm mortar. This sample was ground in the inert-argon atmosphere of a Vacuum Atmospheres Corp. Model HE-43-2 Dri-Lab glovebox in order to rule out moisture pickup as a possible explanation for the effects of grinding. Sample **G3** was less electrostatic than **G1** and **G2** but otherwise showed no visible differences.

Solvated Samples. FeP·CH_2Cl_2. S1. A 32-mg sample of **U1** dissolved quantitatively in ~20 mL of dichloromethane. The solution was heated gently to near boiling and filtered. Hot cyclohexane (~7 mL) was then added through the glass frit. Overnight slow evaporation to dryness produced a beautiful network of purple needles up to 0.5 in. long covering the walls and most of the bottom of the beaker. The Mössbauer run of a portion of this sample was commenced within several hours after evaporation was complete. Subsequently, partial desolvation rendered impossible the characterization of this sample by other techniques.

S2. Sample **S2** was prepared from 223 mg of **U2** in an entirely analogous manner to that described for **S1**. For this preparation, 130 mL of dichloromethane and 45 mL of cyclohexane were employed. Within several hours following evaporation the beaker was covered tightly with Parafilm M and stored in a freezer. The microanalytical results, obtained several weeks later, indicate that this method of storage effectively prevents significant loss of dichloromethane of solvation.

Recrystallization/Desolvated Samples of FeP. D1A. One day following the preparation of the solvated material **S1**, the remaining 13.6 mg not used for the Mössbauer run was vacuum dessicated for 36 h in a drying pistol heated to the boiling point of acetone (56 °C). The observed weight loss of 1.6 ± 0.3 mg corresponds within experimental error to the loss of one molecule of CH_2Cl_2/molecule of FeP. Samples **S1** and **D1A** are visibly indistinguishable from each other.

D1B. In an effort to obtain a less crystalline sample of FeP by *chemical* rather than physical means, 22 mg of the unperturbed sample **U1** was dissolved in ~7 mL of dichloromethane and precipitated rapidly from solution by addition, with agitation, of a large excess (~21 mL) of cyclohexane. Once the fine precipitate had mostly settled, the mixture was centrifuged at high speed for 10 min. The supernatant appeared colorless, indicating essentially quantitative precipitation. The reddish purple solid left behind revealed its microcrystallinity only upon careful scrutiny with an intense flashlight. Vacuum desiccation of **D1B** was carried out exactly as already described for **D1A**.

(2) Supplementary material.

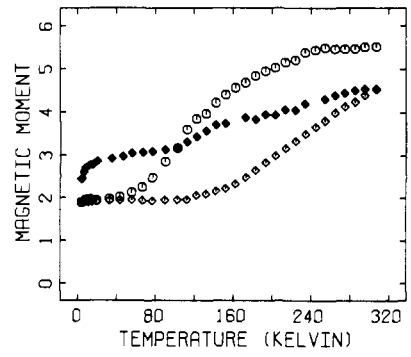

Figure 1. Plots of effective magnetic moment per iron ion, μ_{eff}/Fe, vs. temperature for FeP samples: **U1**, ◇; **S2**, ○; **G1**, ◆.

D2. Vacuum drying of 74.2 mg of **S2** at 56 °C for 36 h resulted in 64.7 mg of **D2**. The measured weight loss of 13 ± 1% agrees well with that calcuated (13.1%) for complete desolvation of FeP·CH_2Cl_2. There was no change in appearance of the sample during desiccation.

Recrystallized/Desolvated Samples, Previously Hand Ground, of FeP. GD1A. About 3–5 mg of material that remained in the mortar used to prepare **G1** was dissolved in ~12 mL of boiling CH_2Cl_2. A 4-mL portion of cyclohexane was added and the unfiltered solution evaporated to dryness overnight. The rather nicely microcrystalline product (smaller crystals than samples **S1** or **S2**) was dried in vacuo for 38 h at 56 °C.

GD1B. After the Mössbauer data collection for **GD1A**, the sample was rinsed from the cell with ~15 mL of dichloromethane. Addition of ~5 mL of cyclohexane to the hot solution was followed by benchtop evaporation. The product, **GD1B**, did not appear as nicely crystalline as other samples crystallized from CH_2Cl_2/C_6H_{12}. In particular, a less easily scraped and redder material was found near the original liquid level on the walls of the beaker. This may be attributed to either (1) smaller particle size, similar to that of the rapidly precipitated sample, **D1B**, or (2) the formation of a less soluble decomposition product. **GD1B** was dried at 56 °C for 36 h in vcuo.

GD3. A 96-mg portion of the sample ground in the argon drybox, **G3**, was dissolved in 60 mL of dichloromethane. The solution was heated to boiling, and 20 mL of warm cyclohexane was introduced. Once more without prior filtration, the solution was slowly taken to dryness. The beautiful purple needles formed in this way were dried at 56 °C in the usual manner. **GD3** strongly resembles **D1A** and **D2** in its phyical appearance.

Results and Discussion

Effects of Solvation. Our familiarity[3] with the influence of lattice imperfections on the *static* properties of spin-crossover solids aroused suspicions that the *dynamic* properties may also be affected. It is well-known that the presence of solvating molecules can dramatically affect the static properties of spin-crossover complexes. Furthermore, FeP forms solvates. We hypothesized that the type **X** samples of FeP, which are prepared by recrystallization from CH_2Cl_2/cyclohexane, differ in the Mössbauer characteristics from the type **U** samples as a result of vacancies created in the desiccation process that removes CH_2Cl_2 molecules of solvation. Our characterization of the solvated compex, sample **S1**, produced some extraordinary results. The properties of the new material FeP·CH_2Cl_2 are described in this section.

The effective magnetic moment (μ_{eff}) vs. temperature curve for sample **S2** is plotted in Figure 1. Experimental data are available in Table II.[2] For purposes of comparison, the corresponding data for the unperturbed microcrystalline sample **U1** are also illustrated in Figure 1. (The data for sample **U2**

(3) (a) Haddad, M. S.; Lynch, M. W.; Federer, W. D.; Hendrickson, D. N. *Inorg. Chem.* **1981**, *20*, 123. (b) Haddad, M. S.; Lynch, M. W.; Federer, W. D.; Hendrickson, D. N. *Inorg. Chem.* **1981**, *20*, 131. (c) Haddad, M. S.; Federer, W. D.; Lynch, M. W.; Hendrickson, D. N. *J. Am. Chem. Soc.* **1980**, *102*, 1468. (d) Haddad, M. S.; Federer, W. D.; Lynch, M. W.; Hendrickson, D. N. *Coordination Chemistry*; Laurent, J. P., Ed.; Pergamon Press: Oxford, 1981; Vol. 21, p 75.

Table IV. Mössbauer Parameters for Sample **S1** of FeP·CH_2Cl_2 (Two-Line Lorentzian Fits)[a]

T, K	CS, mm/s	QS, mm/s	$\Gamma_{1/2}(-)$, mm/s	$\Gamma_{1/2}(+)$, mm/s	ln A[b]	$\chi^2(6)$[c]
299	+0.343 (1)	1.404 (2)	0.379 (2)	0.453 (2)	2.060 (3)	1.30
278	0.361 (1)	1.377 (2)	0.401 (2)	0.487 (2)	2.239 (3)	1.58
247	0.381 (1)	1.312 (2)	0.443 (2)	0.545 (3)	2.472 (3)	5.27
220	0.393 (2)	1.255 (3)	0.501 (3)	0.618 (4)	2.694 (4)	2.44
188	0.383 (2)	1.222 (4)	0.622 (4)	0.712 (5)	2.932 (4)	2.63
175	0.372 (2)	1.273 (4)	0.691 (4)	0.750 (5)	3.025 (4)	1.99
163	0.353 (2)	1.389 (4)	0.779 (5)	0.794 (5)	3.139 (4)	2.09
151	0.330 (2)	1.625 (4)	0.829 (4)	0.805 (4)	3.260 (4)	2.80
141	0.310 (2)	1.885 (5)	0.815 (6)	0.773 (5)	3.362 (6)	5.12
132	0.296 (3)	2.134 (6)	0.731 (7)	0.692 (6)	3.429 (8)	12.3
122	0.295 (3)	2.285 (7)	0.625 (7)	0.587 (7)	3.442 (10)	15.6
108	0.298 (3)	2.405 (6)	0.490 (6)	0.462 (5)	3.422 (10)	184.8

[a] Parameters obtained with assumption of equal areas for the two component peaks of a single quadrupole doublet. Errors in last significant figures are given in parentheses. [b] Natural logarithm of background-normalized area of total fitted spectrum (sum of counts in all channels divided by base line counts). [c] χ-squared value indicating quality of data and of fit to six adjustable parameters.

from which sample **S2** was prepared are very similar.) The solvating CH_2Cl_2 molecule produces a dramatic effect. In comparison to the unsolvated complex, the spin-crossover transition for FeP·CH_2Cl_2 occurs at much lower temperature and proceeds more nearly to completion at the highest temperatures studied. If we define T_c as the temperature at which there are equal populations of high- and low-spin complexes, then T_c for FeP·CH_2Cl_2 (**S2**) is 152.1 K and for FeP (**U1**) is 295.3 K; the difference is 143.2 K. The calculated high-spin fraction of 0.853 at 307.7 K for FeP·CH_2Cl_2 exceeds the maximum value of 0.75 expected for a Boltzmann distribution over the single low-spin Kramers doublet and three high-spin Kramers doublets.

Figure 2 shows the variable-temperature X-band EPR spectra run for sample **S2** of FeP·CH_2Cl_2. The observed trend in relative low- and high-spin signal intensities is consistent with the values for the high-spin fraction obtained from susceptibility data. It is apparent in Figure 2 that very little low-spin population (g = 2 signal at ~3 kG) is evident at 301 K and that the transition is incomplete (i.e., there is still a high-spin signal) at 77 K. In addition to the $g \simeq 4.3$ high-spin signal, there is a low-field shoulder corresponding to $g \simeq 6.3$ visible at temperatures below 174 K; this may indicate the presence of some high-spin site that is less rhombic than the $g \simeq 4.3$ site. Also, the broadening of the components of the rhombic low-spin signal, a phenomenon also observed for unperturbed FeP, occurs at a much lower temperature for FeP·CH_2Cl_2 than for the unsolvated complex. The 4 K EPR signals for **S1** and **U1** are different. The low-spin EPR spectrum of FeP·CH_2Cl_2 covers a significantly larger range of g values (g = 2.355, 2.092, 1.966) than does that (g = 2.314, 2.129, 1.998) for FeP.

It is clear that FeP·CH_2Cl_2 is different from FeP, and not just a mixture of FeP with occluded solvent molecules. Complementary evidence for this assertion is provided by comparisons of infrared spectra and X-ray powder diffraction patterns. The powder X-ray diffraction data for FeP·CH_2Cl_2 are given together with those for FeP in Table III.[2] The pattern for FeP·CH_2Cl_2 is missing the second innermost diffraction ring observed for FeP. Apparently the solvated complex crystallizes in a space group that is similar to but distinct from that for FeP. A strong band observed at ~780 cm^{-1} in unsolvated FeP is missing in the infrared spectrum recorded for FeP·CH_2Cl_2. This band reappears after heating a KBr pellet of FeP·CH_2Cl_2 under vacuum. Other small but real differences are seen between the FeP and Fe·CH_2Cl_2 infrared spectra.

The Mössbauer spectra obtained for the solvated complex bear out its singular identity. Some of the spectra for sample **S1** are displayed in Figure 3. A comparison of the spectra for **S1** with those observed for sample **U1** (see Figure 5 in

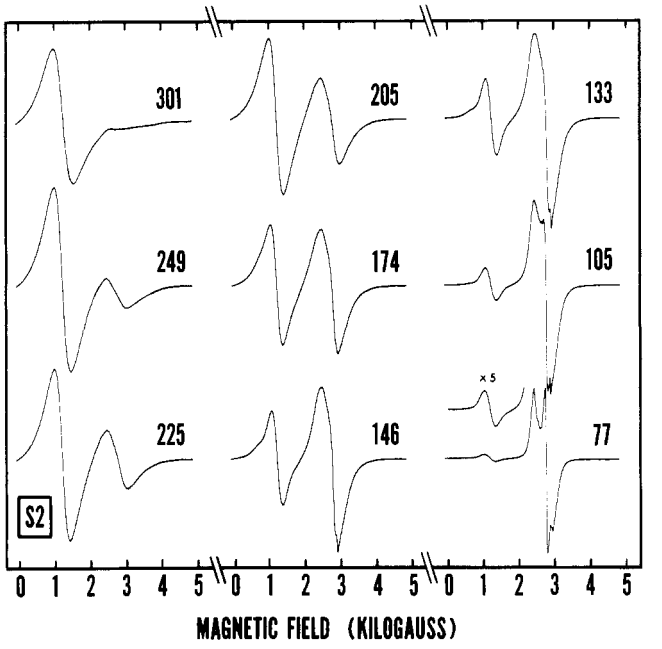

Figure 2. Variable-temperature X-band (9.11-GHz) EPR spectra for sample **S2** of FeP·CH_2Cl_2. Labels correspond to temperatures in Kelvin.

preceding paper) shows that the introduction of the CH_2Cl_2 molecules of solvation leads to pronounced effects. The solvate also seems to be undergoing rather fast low-spin ⇌ high-spin cross relaxation as is seen for **U1** (at least over the temperature range examined for **S1**, 108–299 K); however, the Mössbauer peaks are much broader for **S1** than for **U1**. As with sample **U1**, the **S1** spectra were least-squares fit to two equal-area Lorentzian lines (one quadrupole-split doublet); the resulting fitting parameters are given in Table IV. The least-squares fits (solid lines in Figure 3) follow the data fairly closely for temperatures above 140 K. The deviations between calculated and experimental data for lower temperatures, most visible in the central region of each spectrum, are likely caused by saturation due to finite absorber thickness. Indeed, there is curvature in a plot of natural logarithm of spectral area vs. temperature for sample **S1**; see Figure 4, which also gives data for sample **U1** for comparison. When the high-temperature limiting expression for the Debye model is applied to ^{57}Fe

$$\Theta_M = \frac{E_\gamma}{c}\left[\frac{-3}{M_{eff}k_B\, d(\ln A)/dT}\right]^{1/2} = \frac{11.659}{[d(\ln A)/dT]^{1/2}}$$

the lattice-dynamic parameters can be extracted from the slopes of the linear portions of the curves shown in Figure 4.

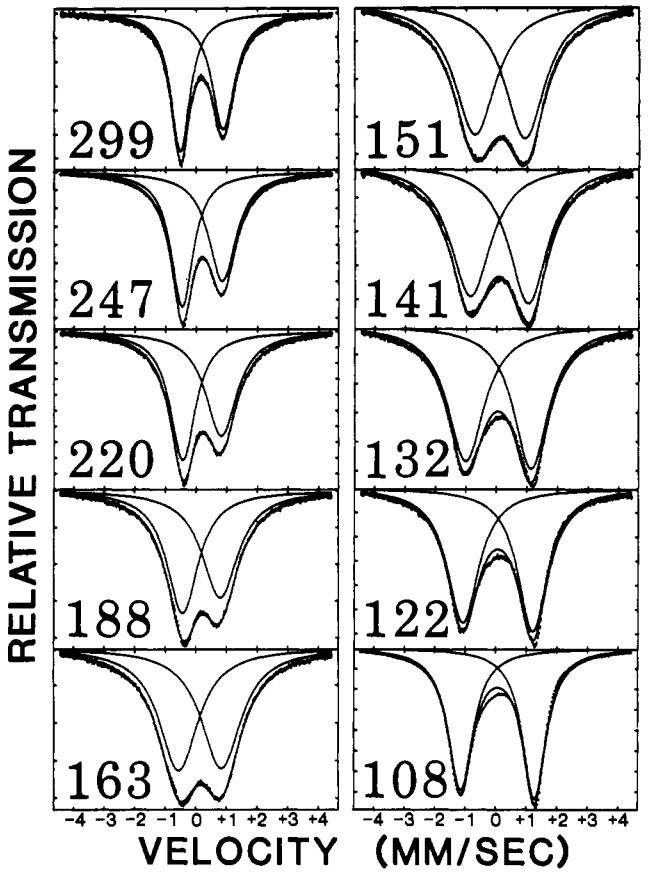

Figure 3. Variable-temperature ^{57}Fe Mössbauer spectra and two-line Lorentzian fits for solvated sample **S1** of FeP·CH_2Cl_2 (absorber concentration 0.78 mg of ^{57}Fe/cm^2). Labels correspond to temperatures in Kelvin.

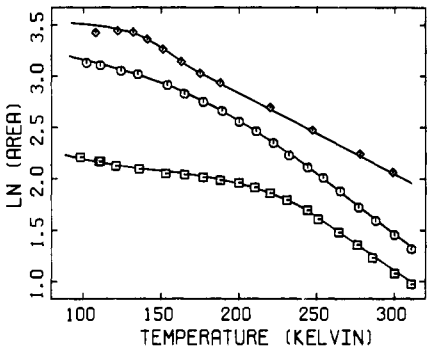

Figure 4. Plots of natural logarithm of background-normalized Mössbauer area vs. temperature: sample **U1** of FeP, □; sample **S1** of FeP·CH_2Cl_2, ◊; sample **G1** of FeP, ○.

The Debye temperature, Θ_M = 131 ± 2 K, found for the solvated sample **S1** is appreciably larger than that found for unsolvated sample **U1**, where Θ_M = 112 ± 2 K. These values indicate (vide infra) that solvation of FeP by dichloromethane molecules strengthens the intermolecular forces. The goodness of linearity of the ln A vs. T plots for FeP (R_{corr} = −0.9995 for all data above 244 K) and FeP·CH_2Cl_2 (R_{corr} = −0.9998 for all data above 188 K) over the temperature interval of the spin-crossover phase transition is somewhat surprising. Apparently the recoilless fractions for high- and low-spin complexes are quite similar.

Figure 5 provides a comparison of the observed trends in line width for each of the two quadrupolar components of the Mössbauer spectra for FeP·CH_2Cl_2 and FeP. There are some similarities in the two data sets. It is intriguing that the maximum line half-width for FeP·CH_2Cl_2 (0.83 mm/s) is about twice as large as that for FeP (0.41 mm/s). The

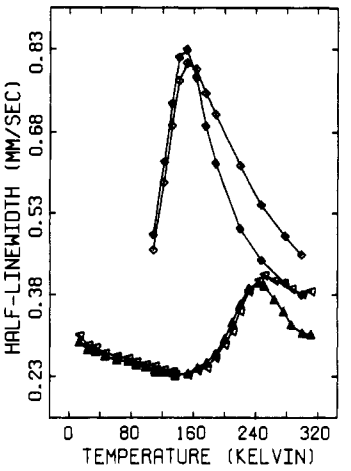

Figure 5. Plots of Lorentzian line half-width vs. temperature for negative and positive velocity components, respectively, of the Mössbauer quadrupole doublets in samples **U1** (▲ and △) and **S1** (♦ and ◊).

presence of a maximum in line width for FeP·CH_2Cl_2 could be attributed to the same origin as that proposed in the preceding paper for FeP—namely that the "spin-flipping" rate is only barely faster than the characteristic Mössbauer frequency. There are at least three explanations for the increased line widths seen at FeP·CH_2Cl_2. First, it is possible that the "spin-flipping" rate in FeP·CH_2Cl_2 is slower than it is in FeP and therefore affects the Mössbauer line shapes more. All other rate-determining factors being equal, a slower rate would be expected for FeP·CH_2Cl_2 *simply because the thermally activated process occurs at a much lower temperature* at which FeP is already completely low spin. Second, at any temperature there are more high-spin complexes present in FeP·CH_2Cl_2 than in FeP. High-spin ferric complexes give intrinsically broader spectra than do low-spin ferric complexes due to relatively slow electronic relaxation. For example, the maximum line half-width for FeP·CH_2Cl_2, 0.83 mm/s for **S1** at 151 K, is considerably less than that for the broadest high-spin component of FeE, 1.4 mm/s at 135 K. There is still ~25% high-spin population at the lowest temperature (108 K) at which the solvate was studied with Mössbauer spectroscopy. Third, it is possible that across the temperature range where FeP·CH_2Cl_2 was studied with Mössbauer spectroscopy there is a distribution of both low- and high-spin sites. For example, at high temperatures a distribution of low-spin nuclei (small regions of molecules) may form, and because of their differences in size (one, two, three, etc. complexes) the low-spin complexes in the different nuclei experience somewhat different lattice forces. This could lead to a distribution in low-spin quadrupole splitting at high temperature.

We have neglected so far to speculate on why solvation of FeP favors the high-spin state. The dramatic influences of solvation on spin-crossover behavior are well-known. Indeed, a recent article by Malliaris and Papaefthimiou[4] has documented the effects of solvation by dichloromethane molecules in the tris(morpholinecarbodithioato)iron(III) system. These authors also find that solvation by CH_2Cl_2 increases the high-spin population; in fact, the solvated dithiocarbamate complex is totally high spin even at 1.45 K. The results of their investigation by Mössbauer spectroscopy, infrared spectroscopy, and magnetic susceptibilities for both solid samples and fluid dichloromethane solutions indicate that the mechanism through which the solvent affects the spin equilibrium does not involve chemical bonding, coordination, or hydrogen bonding between the solute and solvent molecules.

(4) Malliaris, A.; Papaefthimiou, V. *Inorg. Chem.* **1982**, *21*, 770.

Rather, the results of Malliaris and Papaefthimiou indicate that lattice forces are involved. A change in the lattice on going from FeP to FeP·CH_2Cl_2 is indicated by a change in Debye temperature (vide supra). The change in lattice forces may be responsible for the observed increase of *g*-value anisotropy in the low-spin EPR signal upon solvation. Obviously the greater high-spin population in FeP·CH_2Cl_2 at any given temperature could reflect either a lowering in energy of the high-spin excited state or an increase in the energy of the low-spin Kramers doublet ground state, or a combination of both. Our analysis of the *g* values for the low-spin EPR signal suggest that it is a lattice-induced distortion of the low-spin complex such that the low-spin Kramers doublet ground state is raised in energy relative to that of the high-spin excited state (which is an array of three Kramers doublets). In other words, there is likely little change in the crystal field felt by the ferric ion upon solvation, but just a change in the nature of low-symmetry distortion of the low-spin ground state.

Effects of Desolvation. The question still remains as to why there are differences in the physical properties of the types **X** and **U** samples (methods 1 and 2) of FeP. The preparation of the type **X** samples of FeP involves recrystallizing the sample from a CH_2Cl_2/cyclohexane mixture followed by removing the CH_2Cl_2 by heating the solvated FeP under vacuum. It was of interest to see the effect of desolvation on the defect concentration and therefore, presumably, the spin-crossover dynamics in the solid state. The solvated FeP samples **S2** and ^{57}Fe-enriched **S1** were desolvated by heating under vacuum. The resulting materials, samples **D1A** and **D2**, exhibit physical properties nearly identical with those of the unperturbed solids, **U1**, **U2**, and **U3**. Representative EPR and Mössbauer spectra and magnetic susceptibility data for **D1A** and **D2** are given in Figures 6[2] and 7[2] and Tables V[2] and VI.[2] These desolvated FeP samples also give powder X-ray diffraction patterns that are indistinguishable from those for type **U** samples of FeP. All of these experiments indicate that the CH_2Cl_2/cyclohexane recrystallization/desolvation procedure does *not* significantly perturb the spin-crossover behavior of FeP. It appears that if defect structure is indeed responsible for the observed differences between FeP prepared by methods 1 and 2, then the defects are introduced in the initial precipitation from the mother liquor of method 1.

In order to examine further the origin of the defect structure in samples **X1** and **X2**, another recrystallized/desolvated sample, **D1B**, was prepared starting with a portion of unperturbed solid **U1**. The CH_2Cl_2-solvated precursor of **D1B** was isolated *not* by slow evaporation of the solvent mixture but rather by rapid precipitation from a nearly saturated dichloromethane solution by addition of an excess of the nonsolvent cyclohexane. To the eye, the crystallite size looked significantly reduced by this procedure; however, sample **D1B** also demonstrated properties resembling those of an unperturbed solid. In the case of the compound [Fe(3-OMe-SalEen)$_2$]PF_6, which undergoes a very abrupt and complete spin-crossover phase transition, rapid precipitation produced effects similar to grinding of an unperturbed solid.[3b] The above results seem to suggest that the defect structure that affects the spin-crossover transformation is introduced predominantly in the initial precipitation from the mother liquor in the case of samples **X1** and **X2**.

Effects of Grinding. The effects on the *static properties* of spin-crossover complexes of grinding a microcrystalline sample, a process that increases the concentration of defect structure in the crystal fragments, have been established.[3] Will an increase in the defect structure precipitated by compound grinding affect the *dynamics* of the spin-crossover transformation in the solid state? Although a number of ferric tris(dithiocarbamate) complexes that undergo low-spin $\rightleftharpoons$ high-spin interconversion rapidly on the Mössbauer time scale have been shown to be unaffected in their static properties by grinding,[5,6] we have found that FeP does indeed show perturbed behavior upon grinding. As shown in Figure 1, the hand-ground sample **G1** exhibits a more gradual transformation than the corresponding unperturbed sample **U1** as well as a low-temperature plateau at $\sim 2.7\mu_B$ in the effective magnetic moment vs. temperature plot. These susceptibility data indicate that there is a residual high-spin fraction of at least 10% in sample **G1**. As shown in Tables VII[2] and VIII[2], a similar behavior was found for sample **G2**. The magnitude of the observed effect of grinding FeP is comparable to that found by Haddad et al.[3b] for the gradual spin-crossover transition in [Fe(SalEen)$_2$]PF_6.

The influence on the X-ray powder diffraction of grinding samples **U1**, **U2**, and **U3** of FeP was also investigated. The Debye–Scherrer rings observed for the hand-ground samples **G1**, **G2**, and **G3** are invariably more diffuse (i.e., less clearly resolved from the background) than are the corresponding rings for the type **U** samples of FeP, suggesting that grinding produces crystal defects and/or lattice strain.

The effects of grinding **U1** to give **G1** are also readily detected by EPR spectroscopy. Sample **G1** shows a residual high-spin signal at $g \simeq 4.3$ that is about 500 times as intense as that seen for sample **U1** at 4 K. It is interesting that the components of the rhombic low-spin signal for **G1** are also much broader than those for **U1** even at liquid-helium temperature. Once again, the width of the low-spin EPR resonances appears to be directly correlated with the amount of high-spin population. EPR spectra were run over the range of 108–301 K for a third, less vigorously ground sample of FeP, sample **G3**. Comparison of these spectra to those of sample **U3** given in Figure 7 of the preceding paper indicates that grinding increases the high-spin contribution and increases the line widths of the low-spin signal *at all temperatures*. The broadening suggests, whatever its mechanism might be, that *the residual high-spin complexes are indeed randomly distributed within the same crystallites as the majority high-spin complexes and are not in separate domains of any appreciable size*. Their proposed location at crystal defects or surface sites is consistent with all available evidence. The observation of broadening of the low-spin signal with the appearance of residual high-spin complexes also apparently rules out partial sample decomposition to a totally high-spin phase (impurity) as an explanation for the observed behavior (vide infra).

A representative sampling of the many Mössbauer spectra recorded for sample **G1** over the range of 102–311 K is displayed in Figure 8. Clearly, there is a shoulder on the negative velocity quadrupolar component in the spectra measured below 200 K; this feature was not found for the unperturbed FeP sample **U1** (see Figure 5 in preceding paper). The spectra for **G1** clearly must be fit to a sum of at least four Lorentzian peaks (i.e., two doublets). The least-squares fits to two doublets are shown as lines in Figure 8. The fitting parameters are collected in Table IX. For comparison, the parameters for two-line Lorentzian fits (one doublet) of the spectra for temperatures above 200 K are also given in Table X. The four-line fits are satisfactory for all temperatures and offer significant improvements over the two-line fits for all but the very highest temperatures. It can be seen in Figure 8 that the two quadrupole-split doublets have very different temperature dependencies. The components of what is the outer doublet at 102 K collapse inward with increasing temperature until they strongly overlap with the inner doublet. The variation

(5) Albertsson, J.; Oskarsson, A.; Stahl, K. *Acta Chem. Scand., Ser. A.* **1983**, *A36*, 783.
(6) Duffy, N. V.; Lockhart, T. E.; Gelerinter, E.; Todoroff, D.; Uhrich, D. L. *Inorg. Nucl. Chem. Lett.* **1981**, *17*, 1.

Table IX. Mossbauer Parameters for Sample G1 of FeP (Four-Line Lorentzian Fits)[a]

T, K	F(HS)[b]	CS, mm/s	QS, mm/s	$\Gamma_{1/2}(-)$, mm/s	$\Gamma_{1/2}(+)$, mm/s	ln A[c]	$\chi^2(11)$[d]
311	0.5 (4)	+0.39 (5)	1.35 (10)	0.29 (4)	0.55 (8)	1.316 (9)	0.60
		0.29 (1)	1.23 (2)	0.44 (8)	0.35 (6)		
300	0.5 (5)	0.35 (2)	1.25 (4)	0.30 (7)	0.55 (19)	1.453 (9)	0.61
		0.30 (3)	1.27 (6)	0.44 (11)	0.36 (10)		
288	0.5 (5)	0.37 (1)	1.26 (3)	0.33 (6)	0.50 (14)	1.592 (6)	0.68
		0.29 (4)	1.29 (7)	0.38 (4)	0.36 (10)		
277	0.5 (3)	0.39 (1)	1.23 (2)	0.34 (2)	0.48 (4)	1.718 (4)	0.82
		0.27 (2)	1.33 (4)	0.36 (1)	0.37 (3)		
265	0.5 (2)	0.38 (2)	1.20 (4)	0.36 (2)	0.56 (6)	1.879 (6)	0.58
		0.28 (3)	1.43 (5)	0.39 (2)	0.35 (3)		
254	0.66 (8)	0.37 (1)	1.21 (3)	0.37 (1)	0.48 (1)	2.005 (5)	0.62
		0.26 (2)	1.62 (3)	0.36 (2)	0.35 (2)		
244	0.65 (4)	0.36 (1)	1.20 (2)	0.367 (8)	0.460 (8)	2.109 (14)	0.63
		0.27 (1)	1.77 (2)	0.33 (1)	0.34 (1)		
232	0.67 (2)	0.363 (7)	1.24 (1)	0.380 (6)	0.466 (5)	2.224 (3)	0.95
		0.263 (5)	1.90 (1)	0.298 (9)	0.307 (7)		
222	0.66 (2)	0.357 (6)	1.30 (1)	0.405 (4)	0.475 (4)	2.347 (3)	1.81
		0.259 (3)	1.997 (6)	0.281 (6)	0.282 (5)		
211	0.58 (2)	0.36 (1)	1.30 (2)	0.414 (7)	0.496 (6)	2.459 (4)	1.57
		0.261 (3)	2.055 (6)	0.291 (6)	0.283 (5)		
200	0.51 (2)	0.36 (1)	1.29 (2)	0.419 (9)	0.511 (8)	2.555 (4)	2.20
		0.263 (2)	2.116 (5)	0.286 (5)	0.274 (4)		
189	0.47 (2)	0.37 (1)	1.29 (2)	0.45 (1)	0.558 (9)	2.659 (5)	2.38
		0.264 (2)	2.188 (4)	0.274 (4)	0.260 (3)		
177	0.43 (2)	0.37 (1)	1.27 (2)	0.46 (1)	0.58 (1)	2.746 (5)	2.57
		0.265 (1)	2.243 (3)	0.262 (4)	0.250 (3)		
165	0.41 (2)	0.36 (1)	1.29 (3)	0.50 (1)	0.62 (1)	2.826 (6)	2.22
		0.268 (1)	2.294 (2)	0.251 (3)	0.237 (3)		
154	0.41 (2)	0.36 (1)	1.32 (3)	0.55 (1)	0.69 (2)	2.911 (6)	13.7
		0.270 (1)	2.331 (2)	0.242 (3)	0.230 (3)		
135	0.36 (2)	0.36 (2)	1.28 (4)	0.60 (2)	0.81 (2)	3.017 (8)	6.04
		0.274 (1)	2.366 (2)	0.247 (3)	0.236 (2)		
124	0.26 (2)	0.34 (2)	1.073 (5)	0.47 (3)	0.73 (4)	3.050 (7)	3.48
		0.278 (1)	2.391 (2)	0.257 (3)	0.252 (2)		
111	0.23 (2)	0.32 (3)	1.011 (6)	0.48 (3)	0.79 (6)	3.103 (8)	4.13
		0.280 (1)	2.397 (2)	0.258 (3)	0.253 (2)		
102	0.19 (1)	0.32 (2)	0.92 (4)	0.38 (2)	0.69 (5)	3.127 (5)	4.09
		0.288 (1)	2.404 (2)	0.264 (2)	0.261 (2)		

[a] Parameters obtained with assumption of equal areas for the two component peaks of each quadrupole doublet. Errors in last significant figures are given in parentheses. [b] Area fraction of high-spin (inner) doublet. [c] Natural logarithm of background-normalized area of total fitted spectrum (sum of counts in all channels divided by base line counts). [d] χ-squared value indicating quality of data and of fit to 11 adjustable parameters.

Table X. Mössbauer Parameters for Sample G1 of FeP (Two-Line Lorentzian Fits)[a]

T, K	CS, mm/s	QS, mm/s	$\Gamma_{1/2}(-)$, mm/s	$\Gamma_{1/2}(+)$, mm/s	ln A[b]	$\chi^2(6)$[c]
311	+0.330 (2)	1.254 (4)	0.349 (3)	0.427 (4)	1.294 (5)	0.70
300	0.327 (2)	1.247 (3)	0.352 (3)	0.431 (4)	1.433 (5)	0.64
288	0.327 (1)	1.260 (3)	0.362 (2)	0.429 (3)	1.596 (4)	0.72
277	0.330 (1)	1.272 (2)	0.371 (2)	0.432 (2)	1.731 (3)	0.98
265	0.336 (1)	1.311 (2)	0.397 (2)	0.444 (3)	1.883 (4)	0.01
254	0.337 (2)	1.355 (3)	0.419 (3)	0.451 (3)	2.032 (5)	1.64
244	0.338 (2)	1.424 (4)	0.442 (4)	0.461 (4)	2.160 (6)	3.00
232	0.338 (3)	1.508 (6)	0.467 (5)	0.467 (5)	2.293 (8)	7.46
222	0.326 (3)	1.613 (6)	0.487 (6)	0.467 (6)	2.427 (9)	29.6
211	0.316 (4)	1.731 (8)	0.499 (8)	0.464 (7)	2.548 (11)	21.7

[a] Parameters obtained with assumption of equal areas for the two component peaks of a single quadrupole doublet. Errors in last significant figures are given in parentheses. [b] Natural logarithm of background-normalized area of total fitted spectrum (sum of counts in all channels divided by base line counts). [c] χ-squared value indicating quality of data and of fit to six adjustable parameters.

in ΔE_Q for the outer doublet, covering the range of 1.2–2.4 mm/s, is quantitatively very similar to that found for the single doublet of the unperturbed FeP sample **U1**. The center shift for the outer doublet also shows an increase above 220 K. The line widths of the components of the outer doublet increase significantly as well, although no maximum is observed. All these observations indicate that this outer doublet represents a rapidly relaxing spin-crossover species as is present in **U1**. By contrast, ΔE_Q for the inner doublet does *not* show much temperature dependence. All values of ΔE_Q for spectra taken above 130 K are in the range of 1.2–1.3 mm/s. The center shift of this inner doublet also varies little and is larger than that for the outer doublet. The inner doublet has broader lines and is more asymmetric than the outer doublet. At 102 K the contribution from the inner doublet to the total area of the spectrum, 19%, closely matches the residual high-spin fraction calculated from the susceptibility at 102 K, 16%. All of these characteristics for the inner doublet are consistent with its assignment to the residual high-spin complexes that apparently do not participate in the spin-crossover transformation that is fast on the Mössbauer time scale. Whether or not these complexes flip spin at a *finite* but much slower rate cannot

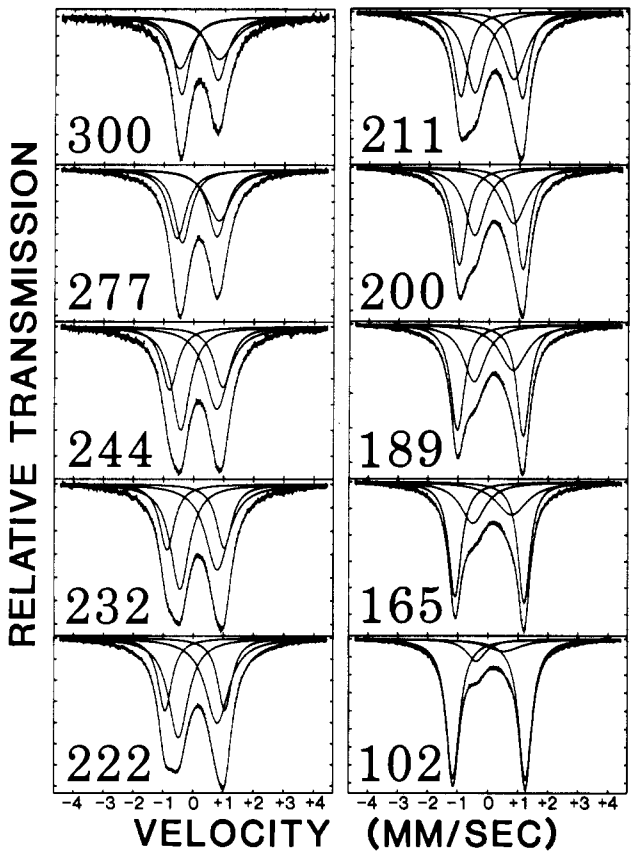

Figure 8. Variable-temperature ^{57}Fe Mössbauer spectra and four-line Lorentzian fits for hand-ground sample **G1** of FeP (absorber concentration 0.87 mg of ^{57}Fe/cm^2). Labels correspond to temperatures in Kelvin.

be determined from the Mössbauer experiment. It must be emphasized that our results indicate that grinding slows down the low-spin ⇌ high-spin interconversion in only *some* of the FeP complexes.

With these exciting new effects of grinding FeP in hand, it became even more important to ascertain that these effects are indeed caused by solid-state factors and are not attributable to sample decomposition. Therefore, we attempted to regain the unperturbed state by recrystallizing sample **G1** from the dichloromethane/cyclohexane solvent mixture. In the first attempt to recrystallize a ground sample of FeP, about 3–5 mg of sample **G1** were recrystallized to give sample **GD1A**. Variable-temperature Mössbauer spectra for **GD1A** showed that some of the residual high-spin complexes had been eliminated. Further recrystallization of **GD1A** produced a poorly crystalline sample **GD1B**. Sample **GD1B** gives a particularly diffuse powder X-ray diffraction pattern. It was concluded that the larger sample of FeP was needed in the recrystallization process to make it effective.

In another attempt at establishing the "reversibility" of the grinding effects, 140 mg of unenriched sample **U3** was ground for ~30 min by mortar and pestle in the argon atmosphere of an inert-atmosphere glovebox. This gave sample **G3**. The EPR data for this ground sample clearly show signals for residual high-spin complexes. The realization of a grinding effect even in the absence of atmospheric moisture and oxygen militates against the possibility of chemical decomposition during the grinding process. Sample **G3** was recrystallized from dichloromethane/cyclohexane, and then the dichloromethane was pumped off to give sample **GD3**. Variable-temperature EPR spectra run for **GD3** were found to be essentially identical with those illustrated in Figure 7 of the preceding paper for the unperturbed sample **U3**. The fact that the grinding damage is indeed reversible was further substantiated

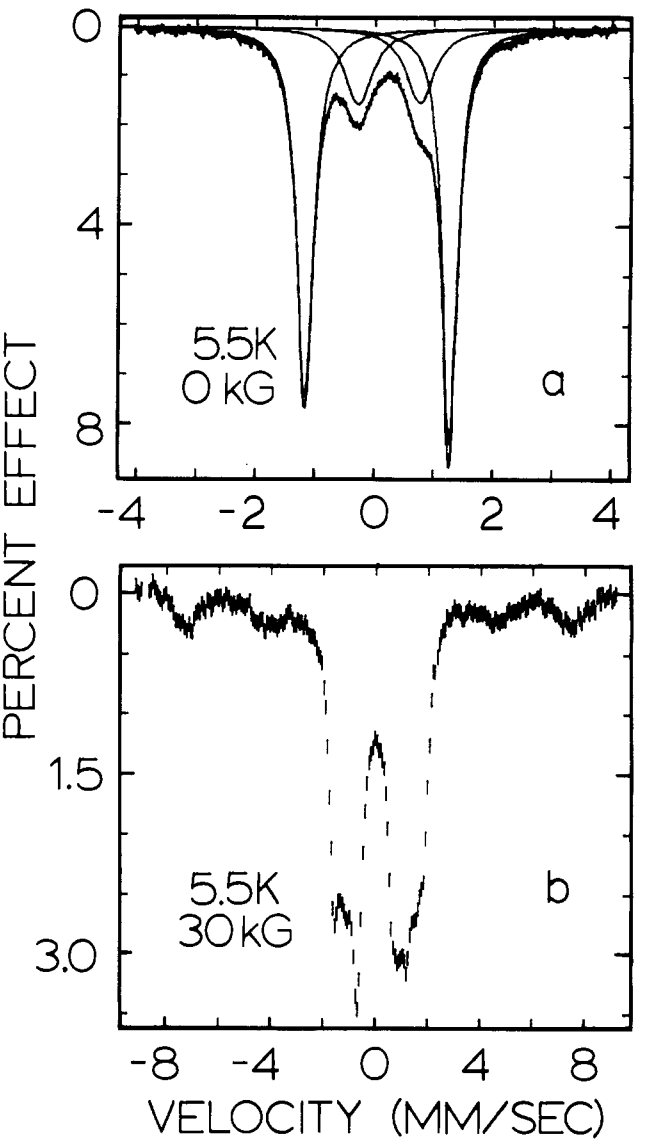

Figure 9. ^{57}Fe Mössbauer spectra of sample **G3** of FeP, which was ground in an inert-atmosphere box: (top) 5 K spectrum in zero field; (bottom) 5 K spectrum in ~30-kG magnetic field.

by comparing Mössbauer spectra for **GD3** with those for **U3**.

Finally, a portion of unenriched sample **G3** was examined with the magnetic Mössbauer technique in order to elucidate further the nature of the two quadrupole-split doublets seen for a ground FeP sample. Figure 9 illustrates the ~5 K zero-field Mössbauer spectrum of **G3**. Clearly visible are two doublets; the inner "residual" high-spin doublet consists of 16% of the spectral area. Also shown in Figure 9 is the spectrum of **G3** at ~5 K with an external magnetic field of ~30 kG. A (broad) magnetic pattern characteristic of a high-spin ferric ion is evident. Thus, it is clear that the inner doublet in the zero-field spectrum is associated with a high-spin ferric complex.

Comments and Conclusions

Considerable physical data have been presented on the ferric spin-crossover complex FeP in "perturbed" states that include a solvated form and a pulverized crystal form. The solvated complex FeP·CH_2Cl_2 is distinctly different from FeP, as indicated by powder X-ray diffraction patterns, and magnetic susceptibility, EPR, and Mössbauer characteristics. Probably the most unusual characteristic of FeP·CH_2Cl_2 is evident in the variable-temperature Mössbauer spectra for this complex. At all temperatures it appears that there is only one quadrupole-split doublet present; however, the two components of each

doublet exhibit *unusually large line widths*. This increased line width reflects either a slower rate of spin-state interconversion in FeP·CH_2Cl_2 compared to FeP or the fact that at any given temperature a sample of FeP·CH_2Cl_2 has a greater percentage of high-spin complexes than does FeP. The desolvation process of eliminating CH_2Cl_2 by mild heating of FeP·CH_2Cl_2 under vacuum does *not* seem to perturb the spin-crossover behavior of FeP; the same observables are found for a desolvated complex as for a microcrystalline sample of FeP prepared in such a way as to not incorporate a solvent molecule.

In this paper the nature of the spin-crossover complexes that give the "shoulders and bumps" seen in the Mössbauer spectra for ground samples of FeP, and for that matter the unperturbed microcrystalline FeP samples (**X** samples in previous paper), was examined. In the case of one pulverized sample the magnetic Mössbauer technique did indicate that the complexes giving the "bumps" in the *5 K zero-field spectrum* are due to high-spin ferric complexes. At this time there is no evidence either for or against the presence of FeP complexes interconverting at an intermediate rate.

In the previous paper no obvious intrinsic (i.e., isolated molecule) factors could be found to explain why FeP flips spin rapidly in the solid state compared to many N_4O_2 ferric complexes. In this paper data for "perturbed" samples of FeP have been presented to show that cooperative solid-state effects may influence the rate of spin-state interconversion. It appears that the low-temperature plateauing phenomenon, found for both "perturbed" compounds and for microcrystalline samples of various spin-crossover complexes, is a manifestation of slow kinetics for the high-spin $\rightleftharpoons$ low-spin transformation. Such behavior is also consistent with a mechanism of nucleation and growth. For all practical purposes the rate of "embryo formation" is equivalent to the spin-flipping rate.

Acknowledgment. We are grateful for support from NIH Grant HL 13652. Partial funding for the Mössbauer equipment came from NSF Grant CHE-78-20727, combined with equal funding from our Chemistry Department and the Research Board of the University of Illinois. We thank Mark Timken for running the 5 K Mössbauer spectra for sample **GD3**, both at zero field and with a 30-kG magnetic field.

Registry No. FeP, 79151-63-6; FeP·CH_2Cl_2, 92219-74-4.

Supplementary Material Available: EPR spectra for **D2** (Figure 6), ^{57}Fe Mössbauer spectra for **D1A** (Figure 7), and listings of microanalytical results (Table I), magnetic susceptibility data (Tables II and VI-VIII), interplanar spacings (Table III), and Mössbauer parameters (Table V) (13 pages). Ordering information is given on any current masthead page.

Contribution from the Department of Chemistry, The University of North Carolina, Chapel Hill, North Carolina 27514

An Electronic Structural Model for the Emitting MLCT Excited States of $Ru(bpy)_3^{2+}$ and $Os(bpy)_3^{2+}$

EDWARD M. KOBER* and THOMAS J. MEYER

Received May 1, 1984

A simple parametric model that includes spin–orbit coupling is developed for the localized MLCT excited states of $M(bpy)_3^{2+}$ (M = Ru, Os). In agreement with experimental data, it is found that there are three closely spaced (<200 cm^{-1}) low-lying states with a fourth state occurring several hundred cm^{-1} to higher energy. As has also been observed, it is predicted that emission from the lowest state is dipole forbidden. Complete state assignments are proposed on the basis of limited polarization data. In general, it is found that, for any Ru or Os bpy complex, no more than four low-lying MLCT states should be present.

Introduction

As a result of extensive applications of the excited states of $Ru(bpy)_3^{2+}$ (bpy = 2,2′-bipyridine) and related complexes as photocatalysts,[1] considerable effort has been expended in attempts to understand the electronic structure of these molecules and particularly of $Ru(bpy)_3^{2+}$ and $Os(bpy)_3^{2+}$.[2-18] The long-term goal of such work is the delineation of those features that control the various excited-state properties.

The relatively long-lived, luminescent excited states of $Ru(bpy)_3^{2+}$ and $Os(bpy)_3^{2+}$ are metal to ligand charge transfer (MLCT) in character,[2] and despite earlier assertions to the contrary,[3] it appears that they can be further characterized as being predominantly triplet states containing an appreciable amount of singlet character as a consequence of spin–orbit coupling.[4,5] The excited-state lifetimes of both complexes are temperature dependent and increase rather dramatically as the temperature is decreased.[6-11] This behavior has been successfully interpreted in terms of a thermally equilibrated Boltzmann population of several low-lying excited states whose lifetimes are temperature independent. Recent measurements

* To whom correspondence should be addressed at the Department of Chemistry, University of Arizona, Tucson, AZ 85721.

(1) (a) Meyer, T. J. *Acc. Chem. Res.* **1978**, *11*, 94–100. (b) Balzani, V.; Bolletta, F.; Gandolfi, M. T.; Maestri, M. *Top. Curr. Chem.* **1978**, *75*, 1–64. (c) Whitten, D. G. *Acc. Chem. Res.* **1980**, *13*, 83–90. (d) Sutin, N.; Creutz, C. *Adv. Chem. Ser.* **1978**, *No. 168*, 1–27. (e) Humphry-Baker, R.; Lilie, J.; Grätzel, M. *J. Am. Chem. Soc.* **1982**, *104*, 422–5. (f) Kalyanasundaram, K. *Coord. Chem. Rev.* **1982**, 46, 159–244.
(2) (a) Klassen, D. M.; Crosby, G. A. *J. Chem. Phys.* **1968**, *48*, 1853–8. (b) Zuloaga, F.; Kasha, M. *Photochem. Photobiol.* **1968**, *7*, 549–55.
(3) (a) Hipps, K. W.; Crosby, G. A. *J. Am. Chem. Soc.* **1975**, *97*, 7042–8. (b) Pankuch, B. J.; Lacky, D. E.; Crosby, G. A. *J. Phys. Chem.* **1980**, *84*, 2061–7.
(4) (a) Felix, F.; Ferguson, J.; Güdel, H. U.; Ludi, A. *Chem. Phys. Lett.* **1979**, *62*, 153–7. (b) Felix, F.; Ferguson, J.; Güdel, H. U.; Ludi, A. *J. Am. Chem. Soc.* **1980**, *102*, 4096–102. (c) Decurtins, S.; Felix, F.; Ferguson, J.; Güdel, H. U.; Ludi, A. *Ibid.* **1980**, *102*, 4102–6.
(5) Kober, E. M.; Meyer, T. J. *Inorg. Chem.* **1982**, *21*, 3967–77.
(6) (a) Hager, G. D.; Crosby, G. A. *J. Am. Chem. Soc.* **1975**, *97*, 7031–7. (b) Hager, G. D.; Watts, R. J.; Crosby, G. A. *Ibid.* **1975**, *97*, 7037–42.
(7) (a) Van Houten, J.; Watts, R. J. *Inorg. Chem.* **1978**, *17*, 3381–5. (b) Van Houten, J.; Watts, R. J. *J. Am. Chem. Soc.* **1976**, *98*, 4853–8.
(8) Allsopp, S. R.; Cox, A.; Kemp, T. J.; Reed, W. J. *J. Chem. Soc., Faraday Trans. 1* **1978**, *74*, 1275–89.
(9) Lacky, D. E.; Pankuch, B. J.; Crosby, G. A. *J. Phys. Chem.* **1980**, *84*, 2068–74.

0020-1669/84/1323-3877$01.50/0